Delivery of Two-Part Self-Healing Chemistry via Microvascular Networks

By *Kathleen S. Toohey, Christopher J. Hansen, Jennifer A. Lewis, Scott R. White,* and *Nancy R. Sottos**

Multiple healing cycles of a single crack in a brittle polymer coating are achieved by microvascular delivery of a two-part, epoxy-based self-healing chemistry. Epoxy resin and amine-based curing agents are transported to the crack plane through two sets of independent vascular networks embedded within a ductile polymer substrate beneath the coating. The two reactive components remain isolated and stable in the vascular networks until crack formation occurs in the coating under a mechanical load. Both healing components are wicked by capillary forces into the crack plane, where they react and effectively bond the crack faces closed. Healing efficiencies of over 60% are achieved for up to 16 intermittent healing cycles of a single crack, which represents a significant improvement over systems in which a single monomeric healing agent is delivered.

1. Introduction

Biological systems rely on pervasive vascular networks to accomplish a remarkable range of functions, including thermal regulation, cellular signaling, and tissue growth and remodeling. The introduction of interpenetrating microvascular networks into synthetic materials enables circulation and delivery of reactive components that can impart bio-inspired functions such as self-cooling, self-sensing and self-healing. Importantly, microvascular delivery of healing agents overcomes a significant limitation of compartmentalized self-healing systems;[1–10] namely, that the supply of healing agent is locally depleted in the latter system after a given damage event, whereas it can be replenished continuously in microvascular-based constructs. Recent optimization analyses of microvascular networks suggest model architectures for healing with minimized impact on structural performance,[11–14] a critical requirement for eventual structural implementation of these concepts.

Toohey et al. recently reported a bio-inspired coating/substrate design[15–17] that delivers healing agent to cracks in a coating via a three-dimensional microvascular network in the substrate (Fig. 1a). A single crack was healed up to seven times with a single, pervasive network. A liquid healing agent consisting of dicylcopentadiene monomer, DCPD, was stored in the embedded network, while a first generation Grubbs' catalyst was mixed directly into the coating to repeatedly heal damage. One drawback of this design was the restricted availability of the solid-phase catalyst, which eventually became depleted upon repeated healing of the

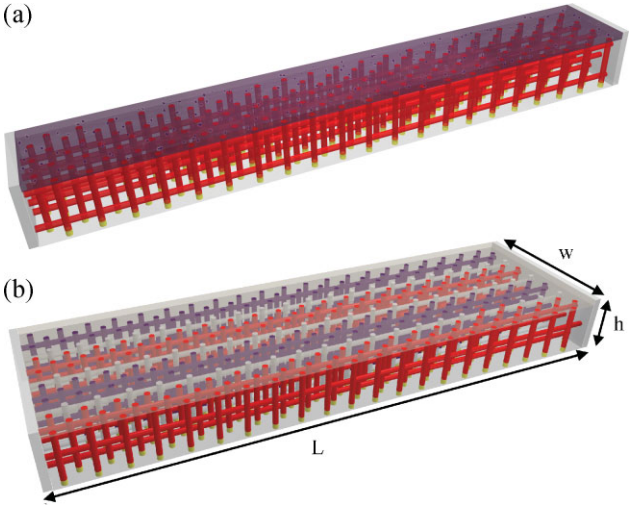

Figure 1. a) Schematic of single network specimen for monomer delivery described in [15]. b) Schematic of a multi-network sample with four independent networks for delivery of a two-part healing chemistry. The red networks represent the resin supply and the purple networks represent the curing agent supply. The resin and curing agent are stored in alternating networks separated by photoblocked regions. Approximate dimensions of samples are $L = 40–45$ mm, $h = 7–9$ mm, and $w = 10–14$mm.

[*] Prof. N. R. Sottos, K. S. Toohey, C. J. Hansen, Prof. J. A. Lewis, Prof. S. R. White
Beckman Institute
University of Illinois at Urbana-Champaign
405 N. Matthews Ave, Urbana, IL 61801 (USA)
E-mail: n-sottos@illinois.edu
Prof. N. R. Sottos, C. J. Hansen, Prof. J. A. Lewis
Department of Materials Science and Engineering
University of Illinois at Urbana-Champaign
1304 W. Green St, Urbana, IL 61801 (USA)
Dr. K. S. Toohey
Department of Bioengineering
University of Illinois at Urbana-Champaign
1304 W. Springfield Ave, Urbana, IL 61801 (USA)
Prof. S. R. White
Department of Aerospace Engineering
University of Illinois at Urbana-Champaign
104 S. Wright St, Urbana IL 61801 (USA)

DOI: 10.1002/adfm.200801824

same crack. This limitation may be obviated by introducing a multi-network architecture for delivery of a two-part epoxy-based healing chemistry.

Williams et al.[18] have developed a vascularized composite sandwich structure that is capable of healing a disbonded interface between the foam core and FRP laminate skin, resulting from impact damage. A full recovery in flexural strength and restoration of primary failure mode was demonstrated using a two-part epoxy healing agent; however, only a single healing cycle was reported. Two-part healing chemistries have also been successfully delivered in microcapsule-based[19,20] and hollow fiber-based self-healing materials,[21–25] providing high healing efficiency for a single healing event.

Here, we report the repeated healing of crack damage in a polymeric coating through delivery of two-part epoxy, healing chemistry via multiple microvascular networks embedded in isolation within a polymeric substrate. We first create a continuous, interconnected microvascular network using the direct-write method developed by Therriault et al.[26] We then isolate multiple networks by infilling the network with a photocurable resin and selectively photopolymerizing thin parallel sections of these resin-filled microchannels. Through this approach, isolated microvascular networks are produced that can independently house different healing agents within the substrate until a crack forms in the coating. Several epoxy and curing agent combinations are evaluated for their suitability in microvascular-based autonomic systems and the two most promising candidates are further evaluated with in situ microvascular healing studies. Repeated healing of a single crack in these coating/substrate architectures is quantified using the experimental protocol developed by Toohey et al.[16] These observations are compared to appropriate controls as well as results from prior work on both compartmentalized and microvascular-based self-healing systems.

2. Results and Discussion

2.1. Two-Part Healing Chemistries

Several two-part, epoxy chemistries were initially screened for their healing ability (Table 1). Optimal chemistries were identified based on their compatibility with the microvascular substrate, low viscosity, and ability to cure under ambient conditions (see Experimental Section for details of the selection process). For example, although all of the resins were compatible with the substrate matrix (EnviroTex Lite, ETI), several curing agent candidates were eliminated due to excessive swelling and/or visible cracking of the microvascular substrate. The viscosity of each healing component influences both its ability to flow through the microvascular network as well as into the crack plane when damage occurs. Two resins with higher viscosities (>1 Pa s) were difficult to infiltrate into 330-μm diameter microchannels, and thus were excluded from further testing. Finally, a simple screening test was conducted to evaluate which combinations of resins and curing agents were capable of curing at ambient temperature with little or no mixing. The resins tested were all bisphenol-A-based (EPON 828) with various diluents; hence, any curing agents that did not cure well with EPON 828 were not tested further. From these observations, the top six combinations (with a rank of 4 or 5 in Table 1) were selected for further evaluation by conducting preliminary in situ healing studies of crack damage in epoxy coatings. Based on the results, only two resin-curing agent combinations, EPON 813 with ANCAMIDE 503 denoted as chemistry A, and EPON 8132 with EPICURE 3046 denoted as chemistry B, were chosen for further testing. Control and in situ tests were conducted on these two chemistry combinations, as described below.

2.2. Control Tests

Control tests were performed with healing chemistries A and B to evaluate the healing performance of each component in the system. Specimens consisted of a brittle epoxy coating on a substrate containing a single microvascular network (Fig. 1a). The specimen was loaded in four-point bending to form a single crack in the coating. In order to ensure a single, unbranched crack, the edge of the coating was notched to create a stress concentration. When a crack formed at the notch, it propagated through the coating and stopped at the coating-substrate interface, enabling the healing agents to wick from the microchannels into the crack plane via capillary action. Previous work showed that the channel openings at the coating-substrate interface attracted the cracks as they propagated down through the coating due to decreased beam stiffness localized at the channel openings.[15] After testing, the specimen was healed for 48 h at 30 °C. By slightly elevating the temperature above room temperature, crack healing was accelerated thereby allowing for a shorter turnaround time between tests. The samples were then reloaded to open the original crack again and to determine if any healing occurred. This process was repeated a total of three times for each specimen.

Two sets of specimens with a single network in the substrate were filled with each of the resins, EPON 813 and EPON 8132, for the two systems studied. The specimens were loaded and healed as described above. For all three loading cycles tested, no healing was observed for either resin. The cracks reopened immediately upon loading after each healing period. As expected, neither of the resins alone was capable of healing a crack in the coating.

Similarly, two sets of curing agent-only control tests were conducted, two with ANCAMIDE 503 and two with EPICURE 3046. The specimens were loaded to initiate a crack and then healed for 48 h, as previously described. Upon reloading after the first healing cycle, the cracks in the coatings healed in one specimen for each of the two curing agents. The healing efficiencies for the single healing cycle in the two successful specimens were 64% for ANCAMIDE 503 (chemistry A) and 81% for EPICURE 3046 (chemistry B). In subsequent healing cycles, no healing occurred for any of the specimens. Healing in the first cycle is attributed to unreacted epoxy groups in the coating, which react with the curing agent delivered to the crack plane to heal the crack for a single cycle.

2.3. In Situ Tests

In situ self-healing tests were performed for specimens that contained chemistries A and B in four independent

Table 1. Two-part healing chemistry screening results ranked by viscosity, matrix compatibility, and curing behavior.

			EPON Resins [a]						
			8021	813 [e]	8132 [f]	815c	8111	8131	828
Curing agents [b]	Viscosity (Pa s)		0.10	0.60	0.60	0.60	0.95	1.4	13
		Matrix Compatibility[c]	y	y	y	y	y	y	y
EPIKURE 3274	0.05	y	0 [d]	4	1	0	1	–	5
EPIKURE 3046 [f]	0.20	y	1	2	4	4	3	–	5
Ancamine K54	0.20	y	–	–	–	–	–	–	0
Ancamide 503 [e]	0.35	y	3	5	5	3	3	–	5
Ancamine 1769	0.60	y	–	–	–	–	–	–	2
Ancamide 2349	0.80	y	3	5	3	0	3	–	5
Sur-Wet R	6.5	y	–	–	–	–	–	–	0
Capcure 3830-81	13	y	–	–	–	–	–	–	0
DETA	0.007	n	–	–	–	–	–	–	–
TETA	0.014	n	–	–	–	–	–	–	–
Jeffamine D-400	0.022	n	–	–	–	–	–	–	–
Jeffamine D-230	0.010	n	–	–	–	–	–	–	–

[a] All resins are EPON 828 with diluents. [b] Curing agents that did not cure with EPON 828 were not tested on the other resins. [c] Matrix compatibility tests (y = yes, n = no). Materials that failed the compatibility test were not tested further. [d] Cure ranking 0 indicates no curing for the resin-curing agent combination and 5 indicates the formation of a solid, brittle polymer. [e] Healing chemistry A: EPON 813 resin, Ancamide 503 curing agent. [f] Healing chemistry B: EPON 8132 resin, EPIKURE 3046 curing agent.

microvascular networks embedded in the substrate. For a given healing chemistry, each individual network was infiltrated with either resin or curing agent in the alternating pattern shown in Figure 1. The two components remained isolated in their respective networks until the coating was cracked. The alternating network pattern contained two regions supplied by resin and two regions supplied by curing agent across the crack plane, resulting in three interfaces where component mixing could occur. Like the controls, specimens were loaded in four-point bending to form a single crack in the coating. After crack formation, specimens were subjected to different types of cyclic loading to enhance fluid flow into the crack and promote mixing of the components. The specimens were healed at 30 °C for 48 h before reloading. The coatings were tested and healed repeatedly until no further healing could be detected. An example of the healing efficiencies from each testing cycle is shown in Figure 2 for the sample that had the best healing performance (III-B).

The first set of in situ specimens was tested with two different healing conditions. Initially, no special conditions were used to promote mixing and healing was allowed to occur purely by diffusion of components within the crack plane. Subsequently, mixing of the components was enhanced by flexing the beam repeatedly by hand 30 times at approximately 2 cycles per second before the 48 h, 30 °C healing period. Multi-network specimens, two for chemistry A (I-A and II-A) and two for chemistry B (I-B and II-B), were prepared and tested as described above. For healing cycles 1–7, only diffusional mixing of the components was allowed and the coatings healed irregularly with only a few successful healing cycles and many unhealed attempts for both chemistry A and B. After healing cycle 7, mixing was enhanced by flexural cycling before the 48-hour healing period. The coatings healed more consistently in the tests following cycle 7 with only a few unsuccessful healing attempts. Tests with no acoustic emission (AE) signal or with inconclusive AE data were assigned a healing efficiency of 0%. The healing efficiencies and number of successful healing cycles for each sample type are shown in Figures 3 and 4. The total number of successful healing cycles is compared to the number of unsuccessful healing attempts in Table 2.

An additional set of specimens (III-A and III-B) was tested with more controlled mechanical loading to promote mixing of the healing components. After loading to form or reopen the crack in the coating, the beam was cycled in the four-point bend fixture at a rate of 40 $\mu m\,s^{-1}$ to a displacement of 20 μm for 50 cycles. After this loading regime, specimens were healed for 48 h at 30 °C. The average healing efficiency of these specimens is provided in Table 2 and plotted in Figure 3. Occasionally, healing efficiencies

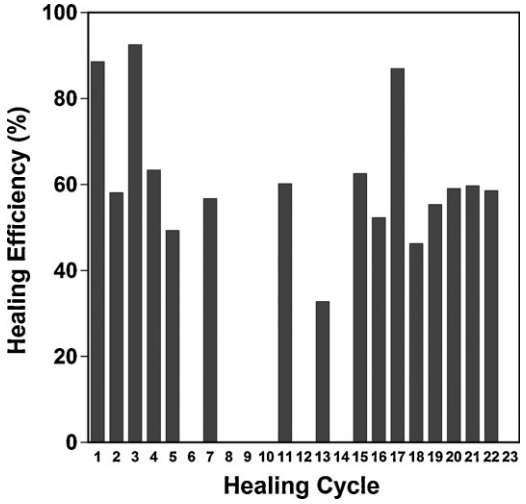

Figure 2. Healing efficiency measured for each cycle of the best performing in situ sample (chemistry B, specimen III). A total of 23 tests were carried out with 16 successful healing cycles.

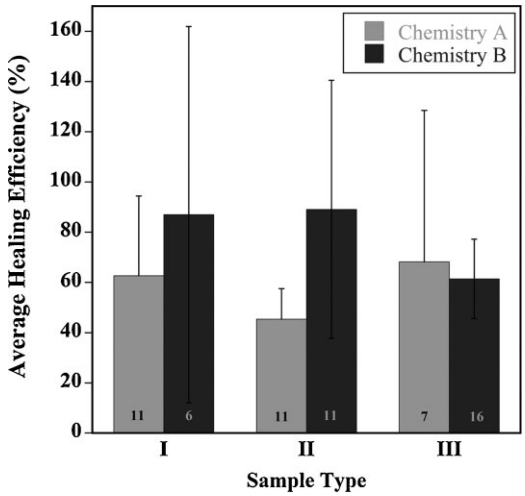

Figure 3. Average healing efficiency of in situ specimens. The successful healing cycles were averaged for each type of specimen for each type of chemistry. The number of cycles included in the average is shown at the bottom of each column.

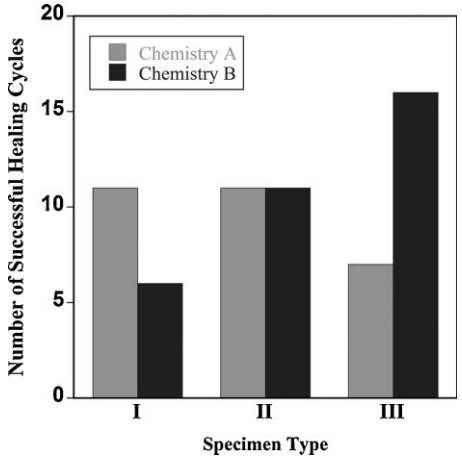

Figure 4. Total number of successful healing cycles for all types of samples tested.

of over 100% were achieved due to excellent compatibility of the healing chemistry and coating materials, as well as increase of the coating toughness upon exposure to healing conditions (30 °C). The initial fracture toughness of the coating was lower since it was originally cured at 21 °C.

2.4. Fractography

After completion of the control and in situ healing tests, the crack planes of all specimens were observed using scanning electron microscopy (SEM). The curing agent-only control and in situ specimens had visible regions of healed material, while the resin-only specimens did not. The appearance of the fracture planes from coatings healed with chemistry A and chemistry B were similar, and are described in more detail below.

Crack surfaces from control samples indicated little to no healing. The crack plane of an unhealed coating from a resin-only control specimen, shown in Figure 5a, possessed a mirror-like finish with no healed material visible. The crack plane of the control specimens with just curing agent had small amounts of

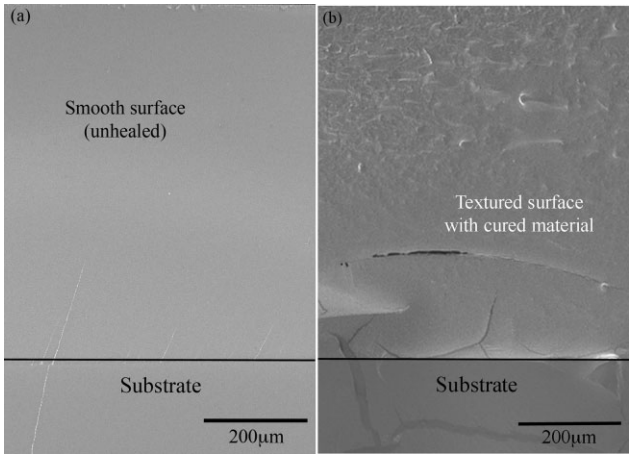

Figure 5. Scanning electron micrographs of control samples. a) Resin-only (chemistry B) sample with a smooth crack plane surface indicative of no healing and b) curing agent-only (chemistry B) sample showing a textured surface on the crack plane resulting from partial healing of the crack.

Table 2. Summary of healing performance of all specimens.

Sample	Chemistry	Mixing Protocol	η_{avg} [±1 sd] (successful cycles)	Cycles with healing	Cycles without healing
I	A	Cycles 1–7 none Cycles 8–16 hand flexing	63 ± 32	11	5
II	A	Cycles 1–7 none Cycles 8–17 hand flexing	45 ± 12	11	6
III	A	Cycles 1–17 controlled flexural cycling	68 ± 60	7	10
Control	A – curing agent only	Cycles 1–2 none	64	1	1
I	B	Cycles 1–7 none Cycles 8–11 hand flexing	87 ± 75	6	5
II	B	Cycles 1–7 none Cycles 8–12 hand flexing	89 ± 51	11	1
III	B	Cycles 1–23 controlled flexural cycling	61 ± 16	16	7
Control	B – curing agent only	Cycles 1–2 none	81	1	1

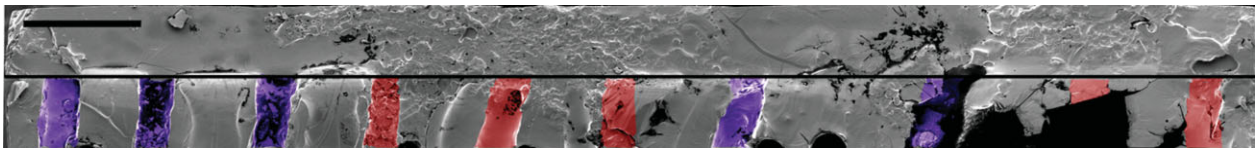

Figure 6. Scanning electron micrographs of the entire crack surface of a sample that healed for multiple cycles using chemistry A. The approximate locations of curing agent channels are shown purple and resin channels are shown in red (Note: These channels are false-colored; scale bar = 1 mm b).

healed material from the first loading cycle, giving the surface a slight texture, as shown in Figure 5b.

By contrast, the crack planes from in situ specimens had significant texture on the surface in the regions above the resin channels. A thick layer of healed polymer developed over these regions, while regions above the channels with curing agent were relatively smooth. A composite image of an entire crack plane was constructed from images acquired along the fracture plane (Fig. 6) for a sample healed with chemistry A. The healed material covered approximately half of the total surface area of the crack plane. However, these localized areas of healing were sufficient to produce high healing efficiencies in specimens for several cycles.

The layer of healed material in the crack plane is shown in Figure 7 under high magnification. Approximately 20 μm of polymerized material appears on one side of the crack face due to build-up of healed material with each successful healing cycle. This deposition of new material in the crack plane with each healing cycle might have eventually blocked the flow of healing components from the microvascular network in the substrate, ultimately preventing further healing.

2.5. Healing Comparison

The supply of two-part healing chemistries via multiple, independent microvascular networks enabled repeated healing events of a single crack in the coating. Up to 16 successful, intermittent healing cycles were achieved with this new delivery method and healing chemistry. By contrast, a microcapsule-based self-healing system consisting of dicyclopentadiene (DCPD) monomer in the capsules and solid phase Grubbs' (first generation) catalyst dispersed in the coating, only exhibited healing for a single cycle.[16] Even our prior microvascular based self-healing coating system, which was comprised of a single network filled with DCPD monomer in the channels and solid phase catalyst (Grubbs' first generation catalyst) embedded in the coating, was only capable of up to 7 repeated healing cycles. In both examples, the finite supply of either the healing agent or catalyst severely limited the number of healing cycles observed.

The ability of the microcapsule, single network, and multiple network delivery platforms to enable repeated healing cycles is highlighted in Figure 8. Healing efficiency of the best performing specimen (most number of healing cycles) from each type of healing system is plotted for the successful healing cycles. The microcapsule specimen with highest healing efficiency contained 10 wt % capsules and 10 wt % wax-protected catalyst (5 wt % catalyst in wax) in the coating.[16] The specimens that relied on monomer delivery through a vascular network exhibited the best performance when 10 wt % Grubbs' catalyst was embedded in the coating.[15] In the current work, the highest number of repeated healing cycles was achieved with chemistry B, subject to controlled mechanical flexural cycling (III-B) to enhance mixing. The delivery of both healing components by this approach led to a dramatic increase in the number of successful healing cycles compared with the capsule-based and single network systems.

2.6. Healing Limitations

Although two-part epoxy chemistries are promising for microvascular based self-healing approaches, a number of limitations remain. A continuous supply of both components for healing was

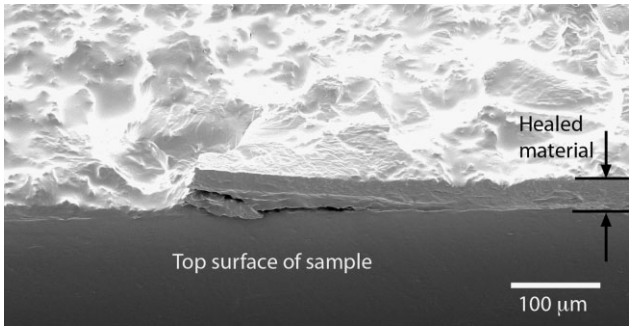

Figure 7. An angled view by scanning electron microscopy of the polymerized material on the crack surface after multiple healing cycles (I-A).

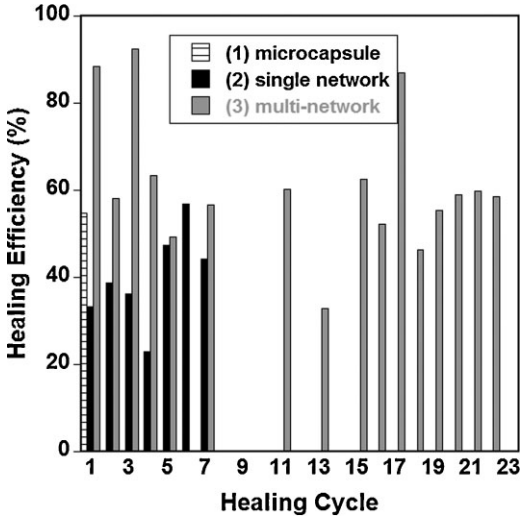

Figure 8. A comparison of healing performance of three types of in situ self-healing coating specimens. 1) Microcapsule: microencapsulated DCPD + first generation Grubbs' catalyst contained in the coating [16]. 2) Single network: a single-network microvascular substrate supplying DCPD with first generation Grubbs' catalyst in the coating [15]. 3) Multi-network: a multi-network microvascular substrate supply of epoxy resin and curing agent (chemistry B) [Note: Only successful healing cycles are shown].

not sufficient to guarantee healing for unlimited cycles. A key issue that contributed to limited healing cycles was mixing of the two components in the crack plane. With no external manipulation of the specimen, the components mix by diffusion alone. Specimens averaged two or three intermittent, successful healing cycles (out of seven attempts) when mixing was solely by diffusion. When specimens were flexed repeatedly to increase flow of the healing components into the crack and to encourage mixing in the crack plane, the coatings healed consecutively for several more cycles. The improved mixing also resulted in an increase in healing efficiencies in some of the specimens. Even with external manipulation to enhance mixing, coverage of healed material in the crack was incomplete, as shown in Figure 6. The location of the healed material (above the resin supply channels) indicates that the fluids in the crack plane did not mix completely and polymerizaton of the healing components was localized. The lowest viscosity component (curing agent) was able to sufficiently migrate to resin-rich areas to initiate polymerization, but the high viscosity resin material did not spread evenly across the crack plane. For regions in which the local supply of resin was starved, the stoichiometry of the mixture was too imbalanced to achieve adequate polymerization and no material was found on the crack face.

Surface tension and non-stoichiometric supply were additional factors that contributed to the localization of the healed material. Relatively high surface tension of the healing components restricted wetting of the crack plane as the components flowed from the channels into the crack. The result was incomplete coverage of the crack surface with the two healing components. The non-stoichiometric ratio (1:1) of the networks in the substrate resulted in an oversupply of curing agent and starvation of resin. The proper stoichiometry for chemistry A was 48 pph curing agent and for chemistry B was 44 pph, or approximately 2:1 resin to curing agent for both chemistries.

Ultimately, the cracks in the coatings stopped healing because the flow and mixing of resin and curing agent was restricted after many successful healing cycles. With each successful healing cycle, the amount of polymerized material in the crack plane increased. The thick build-up of healed material directly above the channels containing resin likely blocked the flow of additional resin into the crack plane in later healing tests. The healed material in the crack also inhibited the ability of the resin and the curing agent to adequately mix.

Design factors such as the spacing of the channels, the diameter of the channels, and the pattern and number of the separate networks within the substrate also impacted the healing. In this work, the present method of creating multiple networks in the beam limited the number of possible networks. Four separate networks were constructed to provide three interfaces for the healing components to mix. More alternations between the resin and curing agent channels along a crack width would provide more interfaces for mixing. Additional networks or sets of alternating channels would also provide ideal stoichiometry of resin to curing agent (2:1) delivered to the crack plane. The ability to create specimens with these features would also require reduced spacing and diameter of the channels, if the overall sample size was held constant. Towards this goal, we are now advancing our direct-write assembly method to enable substrates with embedded, interpenetrating microvascular networks to be produced.[27]

3. Conclusion

Multiple, independent microvascular networks containing a two-component epoxy healing chemistry greatly extended the number of successful healing cycles (up to 16) of cracks in epoxy coatings. The two-part epoxy chemistries demonstrated here possessed the required characteristics for microvascular delivery and autonomic healing including, adequate flow characteristics through the vascular network, chemical compatibility with the substrate matrix material, and autonomic curing within the crack plane after delivery. A combination of direct-write assembly and selective photopolymerization was used successfully to manufacture substrates with four independent microvascular networks that isolated the healing components and released the fluids when triggered by damage. The ability of the two healing components to mix in the crack plane was both an important feature necessary for healing to occur, as well as a limiting factor in attaining more successful healing cycles and higher healing efficiency. Modifications to the design and assembly of the network specimens for two-part healing are underway to further enhance the performance of microvascular-based self-healing materials.

4. Experimental

Two-Part Healing Chemistry: Table 1 is a summary of the screening tests performed on the potential resins and curing agents for healing. The compatibility of potential healing components was examined by placing a representative sample of the substrate in vials and adding one gram of the resin or curing agent. After 48 hours of exposure, swelling of the substrate was quantified by measuring the increase in mass and the material was inspected for embrittlement. Some of the curing agents caused swelling or even severe cracking of the substrate matrix, including triethylene tetramine (TETA), diethylene triamine (DETA), and the polyetheramines Jeffamine D-400 and Jeffamine D-230. These curing agents were eliminated from further screening tests. To test the ability to fill networks with the healing fluids, individual components were placed in a syringe and the fluid was pushed into the open channel end of the network. High viscosity resins (>1 Pa s) were difficult to infiltrate into 330-μm-diameter microchannels. All of the curing agents and the lower viscosity resins were placed in the networks without too much difficulty. Resin-curing agent combinations were tested for curing before in situ testing in the microvascular networks. Approximately 100 μL of resin was placed on a glass slide followed by an equal volume of curing agent. After 24 hours the sample was inspected to determine gel state. Each sample was then slightly mixed by mechanical stirring and allowed an additional 24 hours to cure before the final gel state of the sample was assessed. The resulting polymers from the various combinations of resins and curing agents were ranked according to the degree of gelation. In Table 1, a rank of 0 was assigned to combinations that exhibited no curing, while a 5 indicate that a solid, brittle material formed. Resin-curing agent combinations that were ranked with a 4 or 5 were tested in preliminary in situ tests, and two final combinations were chosen for this study.

Self-Healing Architectures: The specimen geometry was based on the microvascular substrate-coating design used by Toohey et al. [15–17], but instead of a single microvascular network, multiple isolated networks were incorporate in the substrate (Fig. 1b). The substrate was fabricated from a ductile epoxy (EnviroTex Lite, ETI). The coating consisted of twelve parts per hundred (pph) diethylenetriamine (DETA) curing agent (Air Products) and EPON 828 resin (Miller Stephenson). Once mixed and degassed, the uncured coating material was poured into a mold on top of the microvascular substrates. After 22 h of curing at room temperature, the coating was polished to an average thickness of 750 μm.

The microvascular network had a rectangular shape with alternating layers of perpendicular channels to create a face-centered tetragonal geometry [16]. A 330-μm-diameter syringe tip was used to extrude the fugitive ink (60% petroleum jelly and 40% microcrystalline wax), with a center-to-center spacing in each layer of ten times the diameter of the tip. The layers of the network were deposited sequentially until the scaffold reached the desired height. The scaffold was then infiltrated with uncured EnviroTex Lite epoxy. After curing, excess material was cut away, the sides were polished, and the ink was removed by heating and application of light vacuum. The final dimensions of the substrates were approximately 45–50 mm in length, 10–14-mm wide, and 7–9-mm high.

Next, the channel openings on the bottom and sides were blocked, and the network was divided into four separate, parallel networks that ran along the length of the beam (Fig. 1). The channels were filled with an ultraviolet light-sensitive photopolymer (NOA 61, Norland Products). Opaque tape was used to mask the network so that three edges (bottom, front and back) were uncovered. On beams to be used for in situ tests, three longitudinal sections on the top of the beams were also left unmasked. The three sections on the top of the beam created three photoblocked divisions in the original network to produce four independent networks in the substrate. Using a microscope with a mercury source ($\lambda = 365$ nm), the edges and top sections were exposed to UV light to cure the polymer. The remaining uncured resin was removed under vacuum and the channels were rinsed with acetone.

A fugitive wax (Purester 24, Strahl & Pitsch Inc.) was used to fill the channel openings on the top of the substrate to prevent the coating material from penetrating the channels during the application of the coating. The coating epoxy (EPON 828/DETA) was poured onto the top of the microvascular beam in a mold and cured for 22 hours at room temperature (~21 °C). After the coating solidified, the wax was removed by heating (35 °C) and applying a light vacuum. The coating was then polished to the desired thickness.

Mechanical Characterization: Network beams were filled with the appropriate healing components and tested in four-point bending to produce a crack in the virgin test and to reopen the same crack in healing tests. In order to create a single crack in the coating, a razor blade was used to place a notch in the coating. The blade edge was gently pulled across the top corner of the coating producing a stress concentration on the top surface of one side of the coating. The beams were placed in the bending fixture and loaded until a crack formed, or until the original crack reopened. The loading was quickly stopped to prevent additional crack formation. An acoustic emission (AE) sensor (model SE2MEG-P, Dunegan Engineering Company, Inc.) was used for detection of crack initiation or reopening, as described by Toohey et al. [16]. Load–time data, acquired for the loading of the beam, were compared with acoustic event data to determine at what time (and load) the crack formed or reopened. The critical load at crack formation/reopening was used to quantify the degree of healing that occurred in each cycle. The load at the time of crack reopening in a healing test was normalized by the load at the time of crack formation in a virgin test to define the healing efficiency, $\eta = P_{\text{healed}}/P_{\text{virgin}}$ [1,15–17].

Acknowledgements

This work has been funded by the Air Force Office of Scientific Research Multidisciplinary University Research Initiative (Grant # F49550-05-1-0346). K. Toohey was supported in part by the Beckman Institute for Advanced Science and Technology Graduate Fellows Program. C. Hansen is supported in part by an NSF Graduate Student Fellowship. We extend our gratitude to the Imaging Technology Group at the Beckman Institute, especially Scott Robinson, for assistance with scanning electron microscopy.

Received: December 9, 2008
Revised: January 14, 2009
Published online:

[1] S. R. White, N. R. Sottos, P. H. Geubelle, J. S. Moore, M. R. Kessler, S. R. Sriram, E. N. Brown, S. Viswanathan, *Nature* **2001**, *409*, 794.
[2] E. N. Brown, N. R. Sottos, S. R. White, *Exp. Mech.* **2002**, *42*, 372.
[3] E. N. Brown, S. R. White, N. R. Sottos, *J. Mater. Sci.* **2004**, *39*, 1703.
[4] E. N. Brown, S. R. White, N. R. Sottos, *Compos. Sci. Technol.* **2005**, *65*, 2474.
[5] E. N. Brown, S. R. White, N. R. Sottos, *J. Mater. Sci.* **2006**, *41*, 6266.
[6] J. D. Rule, E. N. Brown, N. R. Sottos, S. R. White, J. S. Moore, *Adv. Mater.* **2005**, *17*, 205.
[7] T. C. Mauldin, J. D. Rule, N. R. Sottos, S. R. White, J. S. Moore, *J. R. Soc. Interface* **2007**, *4*, 389.
[8] J. M. Kamphaus, J. D. Rule, J. S. Moore, N. R. Sottos, S. R. White, *J. R. Soc. Interface* **2008**, *5*, 95.
[9] M. R. Kessler, N. R. Sottos, S. R. White, *Composites Part A* **2003**, *34*, 743.
[10] M. M. Caruso, D. A. Delafuente, V. Ho, N. R. Sottos, J. S. Moore, S. R. White, *Macromolecules* **2007**, *40*, 8830.
[11] A. M. Aragón, C. J. Hansen, W. Wu, P. H. Geubelle, J. A. Lewis, S. R. White, *Proc. SPIE-Int. Soc. Opt. Eng.* **2007**, *6526*.
[12] S. Kim, S. Lorente, A. Bejan, *J. Appl. Phys.* **2006**, *100*, 063525.
[13] H. R. Williams, R. S. Trask, A. C. Knights, E. R. Williams, I. P. Bond, *J. R. Soc. Interface 2008*(5), 735.
[14] H. R. Williams, R. S. Trask, P. M. Weaver, I. P. Bond, *J. R. Soc. Interface* **2008**, *5*, 55.
[15] S. Toohey, N. R. Sottos, J. A. Lewis, J. S. Moore, S. R. White, *Nat. Mater.* **2007**, *6*, 581.
[16] K. S. Toohey, N. R. Sottos, S. R. White, *Exp. Mech.* **2008**, online at http://www.springerlink.com/content/p844pj0181x8874/fulltext.pdf.
[17] K. S. Toohey, *Ph.D. Thesis*, University of Illinois at Urbana-Champaign **2007**.
[18] H. R. Williams, R. S. Trask, I. P. Bond, *Smart Mater. Struct.* **2007**, *16*, 1198.
[19] S. H. Cho, H. M. Andersson, S. R. White, N. R. Sottos, P. V. Braun, *Adv. Mater.* **2006**, *18*, 997.
[20] M. W. Keller, S. R. White, N. R. Sottos, *Adv. Funct. Mater.* **2007**, *17*, 2399.
[21] C. Dry, *Compos. Struct.* **1996**, *35*, 263.
[22] J. W. C. Pang, I. P. Bond, *Composites Part A* **2005**, *36*, 183.
[23] J. W. C. Pang, I. P. Bond, *Compos. Sci. Technol.* **2005**, *65*, 1791.
[24] R. S. Trask, G. J. Williams, I. P. Bond, *J. R. Soc. Interface* **2007**, *4*, 363.
[25] R. S. Trask, I. P. Bond, *Smart Mater. Struct.* **2006**, *15*, 704.
[26] D. Therriault, S. R. White, J. A. Lewis, *Nat. Mater.* **2003**, *2*, 265.
[27] C. J. Hansen, K. S. Toohey, W. Wu, S. R. White, N. R. Sottos, J. A. Lewis, *Self-Healing Materials with Interpenetrating Microvascular Networks*, presented at the Proc. for Soc. of Eng. Sci. 45th Ann. Tech. Meeting, Champaign, IL **2008**.